CrossMark

Production of diesel fuel by the hydrotreatment of jatropha oil derived fatty acid methyl esters over γ-Al$_2$O$_3$ and SiO$_2$ supported NiCo bimetallic catalysts

Thushara Kandaramath Hari[1] · Zahira Yaakob[1]

Abstract   γ-Al$_2$O$_3$ and SiO$_2$ supported NiCo bimetallic catalysts were synthesized for the production of diesel fuel by the hydrotreatment of jatropha fatty acid methyl esters (FAME). Upgrading of FAME through hydroprocessing is a sufficient route for improving their characteristics to motor fuel and to overcome their main drawbacks such as oxidative instability, corrosivity and low stability. Hydroprocessing of FAME derived from jatropha oil is more economical and feasible way to produce diesel fuel compared to hydroprocessing of jatropha oil (triglyceride) since the former needs comparatively low hydrogen volumes and reaction pressure. A maximum conversion of 78.2 and 76.1 % were obtained for NiCo/γAl$_2$O$_3$ and NiCo/SiO$_2$, respectively, under the reaction conditions of 2 MPa and 400 °C and straight chain alkanes in the diesel range were the main products. The highest diesel selectivity obtained was 79 and 73 % for NiCo/γAl$_2$O$_3$ and NiCo/SiO$_2$, respectively. As the reaction temperature increased from 300–400 °C, the formation of higher alkanes (>C20) were decreased and formation of lighter alkanes were favored (C8–C16).

Keywords   Diesel fuel · Hydrotreatment · Jatropha fatty acid methyl esters · Supported NiCo bimetallic catalysts

Introduction

Increased environmental pollution and energy crisis increase the demand of production of alternative fuels from renewable resources [1]. At present, biodiesel produced from vegetable oils is used as the transportation fuel, but it has some

✉ Thushara Kandaramath Hari
   thusharahari54@gmail.com

1   Department of Chemical and Process Engineering, Faculty of Engineering and Built Environment, Universiti Kebangsaan Malaysia, 43600 Bangi, Malaysia

disadvantages such as low oxidation stability, high freezing point, low calorific value and low thermal stability [2]. Biomass is one of the most promising renewable resources for the future fuel production. The pyrolysis of biomass is the most used routes for the production of bio oil, but the high oxygen content in the bio oil results in unfavorable fuel properties [3] and so the biooil should be upgraded to improve the fuel properties. Catalytic hydroprocessing is the most suitable route for the conversion of liquid biomass to transportation fuel. Hydroprocessing involves the saturation of double bonds, in the carbon chains of biomass feedstock, removal of hetero atom followed by cracking and isomerization [4]. Grilc et al. performed hydrodeoxygenation and hydrocracking of solvolysed lignocellulosic biomass using oxide, reduced and sulfided $NiMo/Al_2O_3$ catalysts, Ni/Al_2O_3–SiO_2, MoS_2, Pd/Al_2O_3 and Pd/C [5]. They upgraded solvolyzed lignocellulosic biomass by unsupported MoS_2, MoO_2, Mo_2C and WS_2 catalysts at 300 °C and a hydrogen pressure of 8 MPa [6]. They have explained the reaction mechanism and kinetics for hydrotreatment of solvolytically liquefied lignocellulosic biomass using $NiMo/Al_2O_3$ catalyst and developed mass transfer model [7]. Larabi reported the use of nano sized ruthenium or copper–ruthenium supported on heteropolyanion for the production of low oxygenated hydrocarbons from lignocellulosic biomass [8]. Hydroprocessed renewable fuels are hydrocarbon fuels having exactly similar properties of fossil fuels such as carbon chain length, cloud point, calorific value and chemical stability [9].

The conventional hydrotreating catalysts are NiMo or CoMo supported on γ-Al_2O_3. But the main problem with these catalysts is that they must be sulfided with a sulfiding agent to keep the catalyst in the active which would result in sulfur contaminated fuels that cause greenhouse gas emissions and corrosion [10]. Supported noble metal catalysts are highly active for the hydrotreatment process, but their application is not favored on the industrial scale due to their high cost [11]. So recent studies are going on in the search of reduced transition metal catalysts for hydroprocessing. Liu et al. reported the use of $NiMoCe/Al_2O_3$ catalyst for the hydroprocessing of jatropha oil with 80 % hydrocarbon yield of C15–C18 [12]. The hydrotreatment of jatropha oil over $NiMoLa/Al_2O_3$ catalyst is reported with a yield of 78 % and the main product was straight chain alkanes ranging from C15 to C18 [13]. Ni-HPW/Al_2O_3 was used by Liu et al. for the hydroprocessing of jatropha oil to green diesel [10]. Ardiyanti used Ni–Cu bimetallic catalysts supported on a variety of supports such as rice husk carbon CeO_2–ZrO_2, TiO_2, ZrO_2, SiO_2 and Sibunite and observed that $NiCu/TiO_2$ showed the highest activity for the hydrotreatment of fast pyrolysis oil with favorable products [14]. Mohanty et al. performed hydrotreatment of dibenzothiophene and coker light gas oil using NiMo/MAS catalysts synthesized from ZSM-5 nano-clusters [15]. Ni/zeolite catalysts were used for the hydrotreatment of soybean oil and 100 % conversion of soybean oil was obtained at 370 °C, 4 MPa with 74.8 % organic liquid product yield [16]. Pinto et al. carried out the hydrotreatment of pomace oil using $CoMo/Al_2O_3$ and HZSM-5 at a hydrogen pressure of 1.1. MPa and $CoMo/Al_2O_3$ resulted into the maximum alkane yield [17]. Liu synthesized Ni/SAPO-11 catalysts and were used for hydrodeoxygenation of palm oil and the maximum liquid hydrocarbon yield obtained was 80 % [18]. Santillan-Jimenez studied the effect of 20 wt% Ni/C on the catalytic deoxygenation of tristearin and the main products were hydrocarbons in

the range C10–C17 [9]. Monnier et al. used metal nitrides supported on alumina for the hydrodeoxygenation of oleic acid and canola oil at a hydrogen pressure of 7.15 MPa and 380–410 °C [19].

In the present work, we have prepared γ-Al$_2$O$_3$ and SiO$_2$ supported bimetallic NiCo catalyst by co-impregnation method and used for the hydrotreatment of fatty acid methyl esters (FAME) derived from jatropha oil to hydrocarbons. Wang et al. reported the application of Ni-M/γ-Al$_2$O$_3$ (M = Co, Cu, Fe, La) for the hydrodeoxygenation of butanol, butyric acid, methyl ethyl ketone [20]. Upgrading of FAME through hydroprocessing is a sufficient route for improving their characteristics to motor fuel and to overcome their main drawbacks such as oxidative instability, corrosivity and low stability. Hydroprocessing of FAME derived from jatropha oil is more economical and feasible way to produce diesel fuel compared to hydroprocessing of jatropha oil (triglyceride) since the former needs comparatively low hydrogen volumes and reaction pressure. The hydrotreatment of jatropha FAME using NiCo/γ-Al$_2$O$_3$ and NiCo/SiO$_2$ at a hydrogen pressure of 2 MPa produced hydrocarbons in the diesel fuel range. NiCo/γ-Al$_2$O$_3$ and NiCo/SBA-15 catalysts have been reported as excellent catalysts for steam reforming and decomosition of methane [21, 22]. To the best of our knowledge, this is the prime time report of application of alumina and silica supported bimetallic NiCo catalysts for the production of diesel range hydrocarbons. The physicochemical properties of the catalysts were analyzed by X-ray diffraction (XRD), H$_2$-temperature-programmed reduction (H$_2$-TPR), Brunauer–Emmett–Teller (BET) and Barrett–Joyner–Halenda methods (BJH) and Fourier transform infrared spectroscopy (FTIR). The influence of reaction temperature, hydrogen pressure and reaction time on FAME conversion and diesel selectivity were studied.

Experimental

Catalyst preparation and characterization

NiCo/γ-Al$_2$O$_3$ and NiCo/SiO$_2$ catalysts were prepared by the co-impregnation method using an aqueous solution having both the metal precursors Ni(NO$_3$)$_2$·6H$_2$O and Co(NO$_3$)$_2$·6H$_2$O [21]. For the synthesis of NiCo/γ-Al$_2$O$_3$, to 400 ml of the aqueous solution containing both Ni(NO$_3$)$_2$·6H$_2$O and Co(NO$_3$)$_2$·6H$_2$O, 20 g of γ-Al$_2$O$_3$ support (60 mesh, acidic, Alfa Aesar chemicals) was added slowly and impregnated to dryness. The loading of Ni and Co were kept at 10 wt% each. After impregnation, the catalyst was dried at 90 °C for overnight and calcined at 500 °C for 4 h. A similar procedure was used for the synthesis of NiCo/SiO$_2$ using SiO$_2$ (200 mesh, Sigma Aldrich) as support.

The crystalline phase of the catalysts was examined using Bruker AXS D8 Advance diffractometer with Cu K$_\alpha$ radiation having a wavelength of 0.15406 nm in the 2θ range 3–80° with a scan speed of 0.025°/s. Fourier transform infrared spectrum (FTIR) was recorded on a Nicolet 370 FTIR spectrometer in the range of 400–4000 cm^{-1} with 10 average scans and a resolution of 4 cm^{-1}. The surface area and pore size distribution were measured using BET and BJH methods by measuring N$_2$ adsorption–desorption isotherms at 77 K with a Micrometrics ASAPE

2010 system. The samples were degassed at 350 °C for 4 h. The reducibility of the catalysts was studied by temperature programmed reduction (TPR) using 10 % hydrogen, nitrogen mixture with a flow rate of 20 ml/min and 10 °C/min heating rate up to 600 °C in a Micromeritics Autochem 2920 analyzer.

Catalytic activity studies

The HDO activity of the catalyst was studied in gas phase fixed bed reactor. In each run, 2 g catalyst was loaded into the reactor and the catalyst was reduced at 400 °C for 3 h under H_2 flow of 100 ml/min at atmospheric pressure [23, 24]. After reduction, the reaction pressure was increased to 2 MPa and jatropha FAME (diluted 10 times with n-heptane) was pumped into the reactor at a flow rate of 16 ml/h after preheating at 300 °C. The reaction temperature was varied for 300–400 °C at an interval of 50 °C. H_2/feed ratio was 375 ml/ml of oil. The liquid products of the reaction were analyzed with a GC-2014C Shimadzhu gas chromatograph with DB-1 (60 m × 0.32 mm × 1 μm) capillary column and a FID detector. N_2 was used as carrier gas and sample injection was performed in split mode with a split ratio 24.6. The temperature program was started from 50 °C and the column temperature was increased to 320 °C with a heating rate of 10°/min and the temperature was maintained at 320 °C for 13 min. Gaseous products were analyzed to identify the components and to study the reaction pathway. The conversion of FAME and selectivity of diesel range hydrocarbons was calculated based on GC data.

$$Conversion\ (\%)$$
$$= \frac{Concentration\ of\ FAME\ inget\ - Concentration\ of\ FAME\ in\ outlet}{Concentration\ of\ FAME\ in\ inget} \times 100$$

$$Diesel\ Selectivity\ (\%) = \frac{Concentration\ of\ diesel\ range\ products\ (C12-C20)}{Concentration\ of\ total\ organic\ liquid\ products} \times 100$$

Results and discussion

Catalyst characterization

The X-ray diffraction patters of NiCo/γ-Al$_2$O$_3$ and NiCo/SiO$_2$ are shown in Fig. 1. For NiCo/γ-Al$_2$O$_3$ catalyst, characteristic diffraction patterns of alumina support were observed at 2θ = 31.2°, 36.6°, 44.8° and 67.4°. The presence of cubic cobalt oxide (Co_3CO_4) was detected due to characteristic diffraction peaks at 2θ = 19°, 31.2°, 36.8°, 44.8°, 59.3° and 65.2°. The presence of nickel oxide (NiO) was also detected at 2θ = 37.3°, 43.2°, 62.8°, 75.5° and 79.1°. In addition, cobalt aluminate ($CoAl_2O_4$) and nickel aluminate ($NiAl_2O_4$) were also detected and identified from the XRD pattern. Some of the diffraction peaks of cobalt aluminum oxide, cobalt oxide, nickel aluminum oxide and alumina were found to be overlapped [21, 25] but
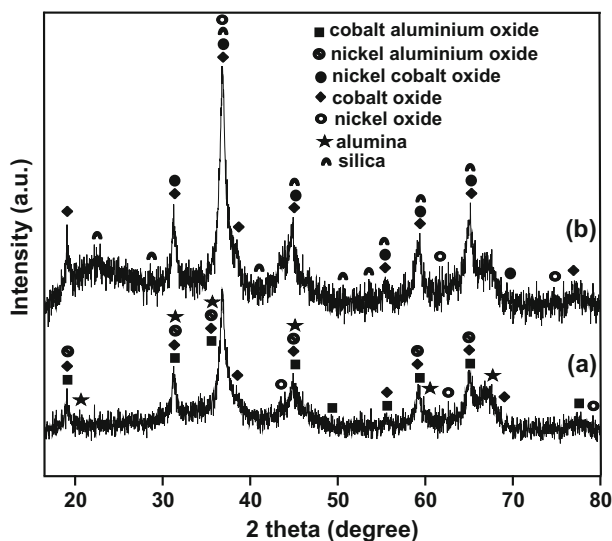
Fig. 1 X-ray diffraction patters of NiCo/γ-Al$_2$O$_3$ (*a*) and NiCo/SiO$_2$ (*b*)

their existence was confirmed by the presence of other individual diffraction peaks. Considering NiCo/SiO$_2$, the characteristic diffraction patterns of spinel cobalt oxide (Co$_3$CO$_4$) were detected at 2θ = 18.9°, 31.2°, 36.8°, 44.7°, 55.6°, 59.2°, 65.1°, 77.2°. The diffraction patterns of rhombic NiO were observed at 2θ = 37°, 62.1°, 74.5°, 78.3°. The presence of cubic nickel cobalt oxide (NiCo$_2$O$_4$) was detected at 2θ = 31.1°, 36.7°, 44.6°, 55.4°, 59.1°, 64.9°, 69.4°, which was not found in the diffraction pattern of NiCo/γ-Al$_2$O$_3$. The diffraction patterns of orthorhombic SiO$_2$ support were also detected. A few peaks of nickel cobalt oxide, cobalt oxide and silica overlapped, which makes the quantitative of individual phases quite difficult. The crystallite sizes of both the catalysts were calculated based on the Scherrer formula and found to be 12.5 nm and 13.3 nm for NiCo/Al$_2$O$_3$ and NiCo/SiO$_2$, respectively. X-ray fluorescence spectral studies of the catalysts, Ni:Co atomic ratios were found to be 1:1.12 and 1:1.11 for NiCo/Al$_2$O$_3$ and NiCo/SiO$_2$, respectively.

Fig. 2 shows FTIR spectra of NiCo/γ-Al$_2$O$_3$ (a) and NiCo/SiO$_2$ (b). Peaks due to characteristic metal–oxygen bond stretching vibrations were observed in the region 685–690 cm^{-1}, 442–475 cm^{-1} and 569–585 cm^{-1}. Vibrations in the region 685–690 cm^{-1} characteristically show the presence of bridging metal–oxygen bond. A peak at 1060 cm^{-1} due to the presence of the terminal oxygen was clearly observed in the case of NiCo/SiO$_2$. For NiCo/γ-Al$_2$O$_3$, all the corresponding peaks were not individually resolved, but appeared as a wide band.

The temperature programmed reduction profiles of NiCo/γ-Al$_2$O$_3$ (a) and NiCo/SiO$_2$ (b) are shown in Fig. 3. The TPR profile of NiCo/γ-Al$_2$O$_3$ contains five reduction peaks at 310, 338, 405, 475 and 535 °C. The peaks in the range 300–450 °C are assigned to three main reduction processes, (1) reduction of NiO to Ni, (2) two-step reduction of Co$_3$Co$_4$ to CoO and then to Co. The other reduction peaks beyond 450 °C correspond to the reduction of NiAl$_2$O$_4$ and CoAl$_2$O$_4$. Under
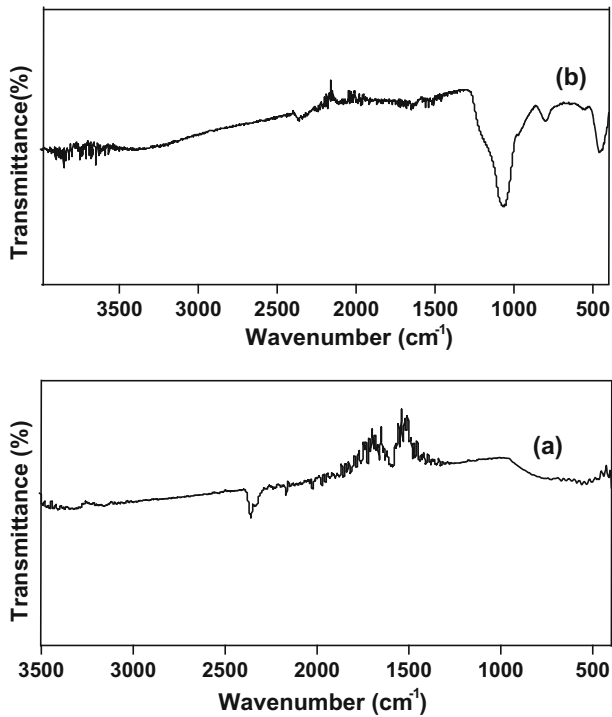
Fig. 2 FTIR spectra of NiCo/γ-Al$_2$O$_3$ (**a**) and NiCo/SiO$_2$ (**b**)
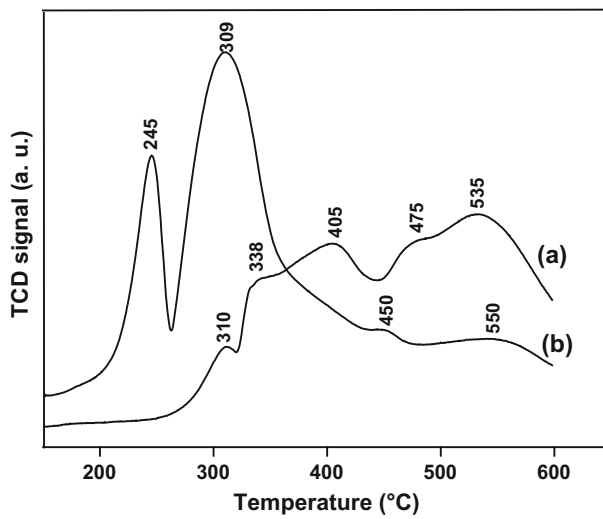
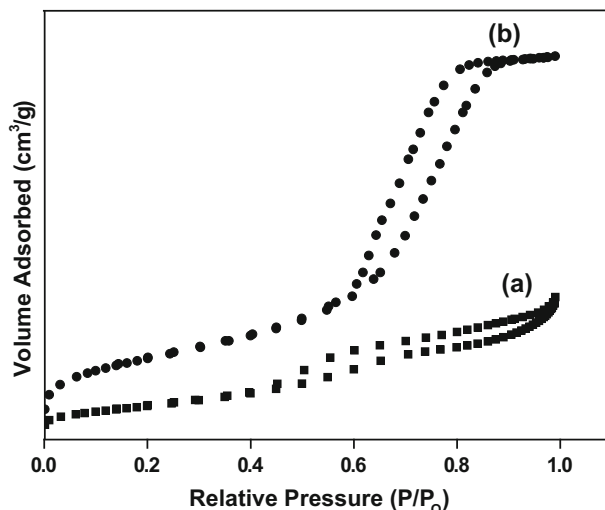**Fig. 3** TPR profiles of NiCo/γ-Al$_2$O$_3$ (*a*) and NiCo/SiO$_2$ (*b*)

Fig. 4 N_2 adsorption–desorption isotherms of NiCo/γ-Al$_2$O$_3$ (*a*) and NiCo/SiO$_2$ (*b*)

the present reaction conditions, the active species present in the catalyst are expected to Ni^0 and Co^0 emerged as the result of reduction of NiO and Co$_3$Co$_4$. Considering NiCo/SiO$_2$, two sharp peaks were observed at 245 and 309 °C and two broad peaks at 450 and 550 °C corresponds to reduction of NiO, Co$_3$Co$_4$ and NiCo$_2$O$_4$ [26–28].

According to the surface area and pore size distribution studies using N_2 adsorption–desorption isotherms, NiCo/γ-Al$_2$O$_3$ had a surface area of 114.8684 m^2/g and showed type 4 adsorption–desorption isotherm with H4 hysteresis loop (Fig. 4). For NiCo/SiO$_2$, the BET surface is found to be 270.9973 m^2/g. Type 4 adsorption–desorption isotherm was exhibited by NiCo/SiO$_2$ with H2 hysteresis. NiCo/γ-Al$_2$O$_3$ showed mono modal pore size distribution and had a pore volume 0.215128 cm^3/g with average pore size 51.543 Å while NiCo/SiO$_2$ showed multi modal pore size distribution with an average pore volume of 0.573677 cm^3/g and average pore size 62.801 Å (Fig. 5).

Hydroprocessing of jatropha fatty acid methyl esters

Tables 1 and 2 show the specifications of FAME used in this study. Since temperature plays an important role in the hydrotreatment process, we have studied the effect of temperature on reactant conversion and also on desired product selectivity. From Fig. 6, it can be observed that the maximum conversion was obtained at 400 °C for both NiCo/γ-Al$_2$O$_3$ and NiCo/SiO$_2$. In the case of NiCo/γAl$_2$O$_3$, the maximum conversion was 78.2 %, and for NiCo/SiO$_2$ it was 76.1 %. As the temperature increases from 300 to 400 °C, the selectivity of diesel range hydrocarbons (C12–C20) increased for both the catalysts (Fig. 7). An increase in the reaction temperature decreased the formation of higher hydrocarbons (>C20), but favored the formation of hydrocarbons of jet fuel range (C8–C16) mainly by
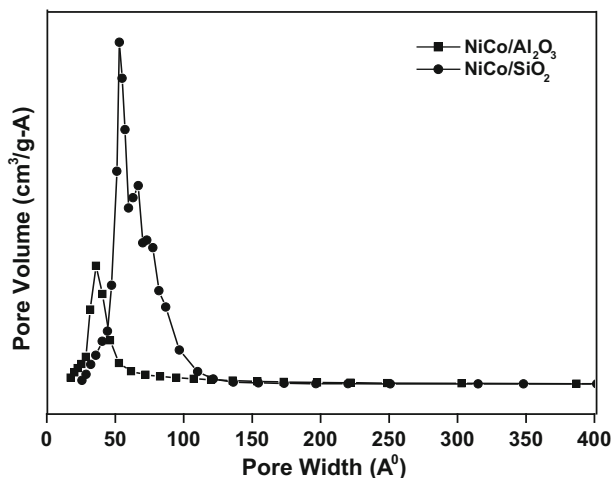
Fig. 5 BJH pore size distribution plots of NiCo/γ-Al$_2$O$_3$ (*a*) and NiCo/SiO$_2$ (*b*)
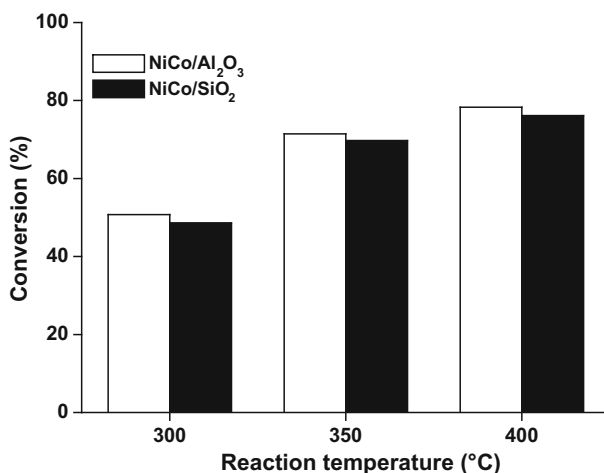

Fig. 6 Effect of reaction temperature on conversion at H$_2$ pressure = 2 MPa, feed flow rate = 16 ml/h, H$_2$/Feed ratio = 375 ml/ml

hydrocracking [12]. The major components in the product are straight chain alkanes mainly C15–C18 hydrocarbons. The maximum diesel selectivity was obtained at 400 °C for both the catalysts. A maximum diesel selectivity of 79 % was obtained for NiCo/γ-Al$_2$O$_3$ and 73 % for NiCo/SiO$_2$. Moreover, carbon dioxide and methane were the main components detected in the gaseous products.

The influence of reaction pressure on the conversion of FAME and diesel selectivity was studied by varying the hydrogen pressure from 0.5–2 MPa and the results are shown in Fig. 8. When the reaction was carried out at a reaction pressure of 0.5 MPa, the conversion was very low (<10 %) in the case of both the catalysts.
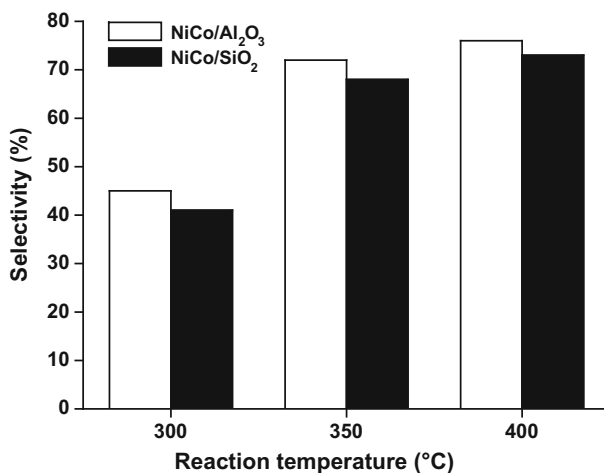
Fig. 7 Effect of reaction temperature on selectivity of diesel range hydrocarbons at H_2 pressure = 2 MPa, feed flow rate = 16 ml/h, H_2/Feed ratio = 375 ml/ml
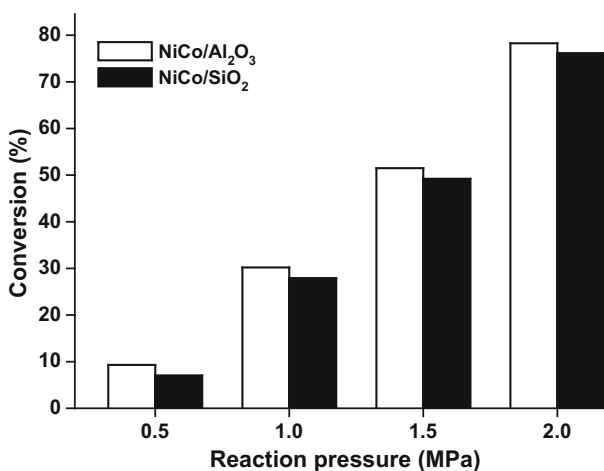

Fig. 8 Effect of reaction pressure on conversion at temperature = 400 °C, feed flow rate = 16 ml/h, H_2/ Feed ratio = 375 ml/ml

As the increase in pressure from 0.5 MPa to 2 MPa, a considerable and sudden increase in the FAME conversion was obtained. At 2 MPa, the FAME conversion obtained for NiCo/γ-Al_2O_3 was 78.2 % and diesel selectivity was 79 %, while for NiCo/SiO_2 it was 76.1 and 73 %, respectively (Fig. 9).

Based on the product distribution results, the hydrotreatment of jatropha FAME were expected to proceed through two pathways mainly, hydrodeoxygenation and hydrodecarboxylation/hydrodecarbonylation. Hydrocracking was the other possible reaction route to consider. Fig. 10 shows a plausible pathway for the hydrotreatment
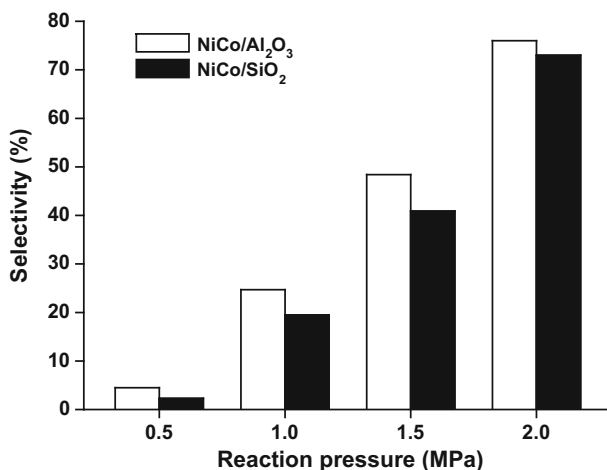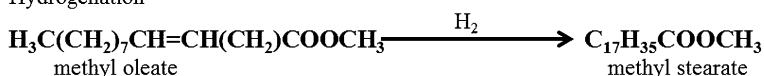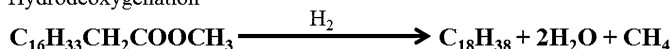
Fig. 9 Effect of reaction pressure on selectivity of diesel range hydrocarbons at temperature = 400 °C, feed flow rate = 16 ml/h, H_2/Feed ratio = 375 ml/ml
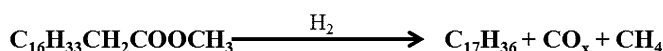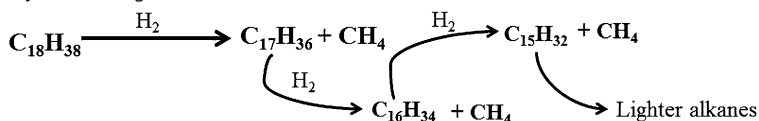

Fig. 10 The plausible deoxygenation pathways in hydrotreatment of FAME using methyl oleate as model compound

of FAME derived from jatropha oil, methyl oleate as model compound. The major products of hydrodeoxygenation are C18 and C16 and hydrodecarboxylation/hydrodecarbonylation route results mainly in the formation of C15 and C17 hydrocarbons. For both NiCo/γAl$_2$O$_3$ and NiCo/SiO$_2$, the major products formed were C15–C18 hydrocarbons and so it can be concluded that the deoxygenation proceeded through both hydrodeoxygenation and hydrodecarboxylation/hydrodecarbonylation pathways. With an increase in the reaction temperature from 300 to
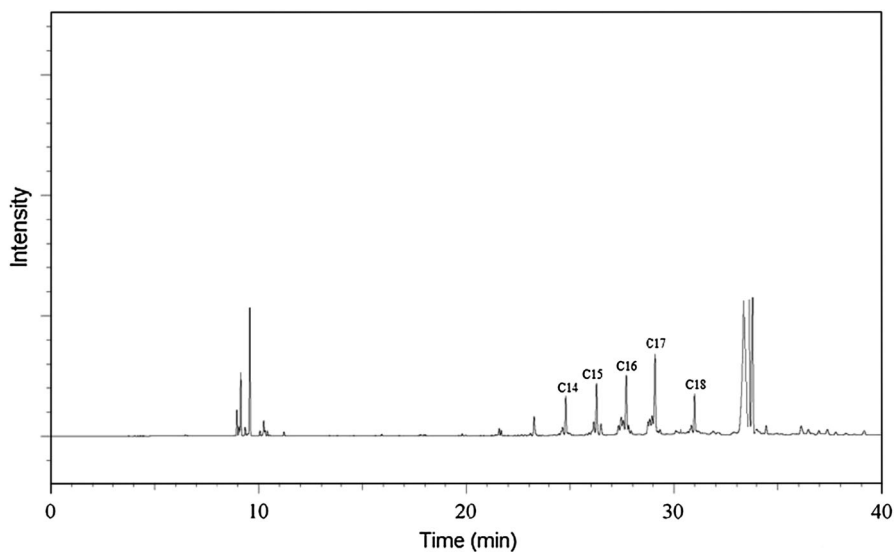
Fig. 11 Gas chromatogram of the hydrotreated jatropha oil derived FAME products obtained with NiCo/γ-Al$_2$O$_3$ catalyst at 400 °C

400 °C, hydrocracking route became more significant which resulted in lighter products. Fig. 11 shows the GC chart of liquid product distribution obtained for hydroprocessing of NiCo/γ-Al$_2$O$_3$. The higher activities of the supported NiCo catalysts are expected due to smaller crystallite size (12.5 and 13.3 nm for NiCo/Al$_2$O$_3$ and NiCo/SiO$_2$, respectively) and higher surface area that which increase the number of exposed metal atoms and the combined effect of Ni and Co metals [21, 26]. Oxygen atoms of the FAME get adsorbed on the surface of the catalyst.
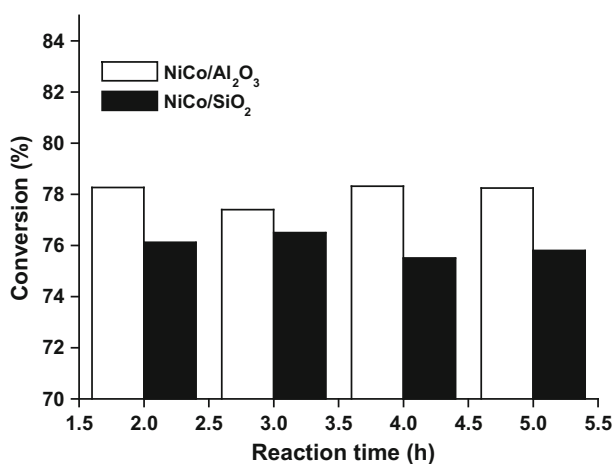

Fig. 12 Effect of reaction time on conversion at H$_2$ pressure = 2 MPa, feed flow rate = 16 ml/h, H$_2$/Feed ratio = 375 ml/ml, reaction temperature = 400 °C
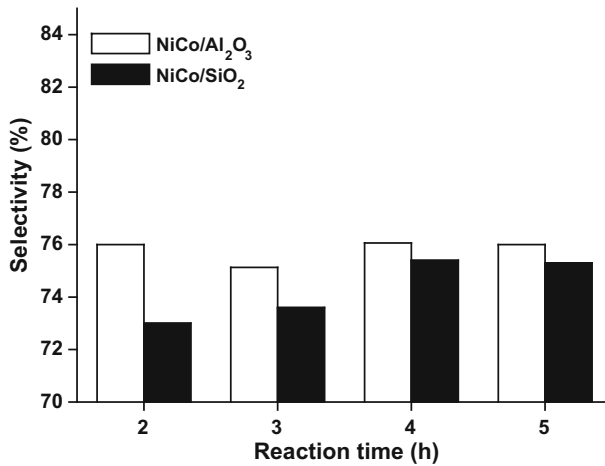
Fig. 13 Effect of reaction time on selectivity of diesel range hydrocarbons at H_2 pressure = 2 MPa, feed flow rate = 16 ml/h, H_2/Feed ratio = 375 ml/ml, reaction temperature = 400 °C

Table 1 Properties of jatropha oil derived FAME

Properties	Method	Jatropha biodiesel
Density (kg/m^3, 15 °C)	ASTM D4052	877.5
Viscosity (mm^2/s, 40 °C)	ASTM D445-04	3.6
Acid value (mg KOH/g)	ASTM D664	0.34
Flash point (°C)	ASTM D92-05a	225
Moisture content (%, w/w)	ASTM D6304	0
Sulfur content (%, w/w)	ASTM D4294	0

Different oxygen atoms on the FAME adsorb on different sites of the catalyst and comparatively alumina support more facilitates the interaction of oxygen atoms because of the presence of more acidic OH sites. Reduced metals activated H_2 and H_2 spills over to adsorbed oxygen of the FAME resulting C-O bond cleavage.

The effect of reaction time on the conversion of jatropha FAME was studied using both the catalysts continuously for 5 h and the results are shown in Fig. 12. From the results, it can be observed that the conversion was apparently constant during the complete course of the reaction. Diesel fuel selectivity also remained almost constant with increase in time up to 5 h (Fig. 13). Table 3 shows a

Table 2 Fatty acid methyl ester composition of FAME

Fatty acid methyl ester	Weight (%)
Palmitic 16:0	14.85127
Stearic 18:0	7.23671
Oleic 18:1	38.78608
Linoleic 18:2	38.16238
Others	0.9635

Table 3 Comparison of the catalytic activity and reaction conditions of present catalysts with literature reports

Catalyst	Feed	Reaction temperature (°C)	Reaction pressure (MPa)	Maximum conversion (%)	Ref.
Ni-HPW/Al_2O_3	Jatropha oil	300–380	3.3	99.85	[10]
NiMoLa/Al_2O_3	Jatropha oil	280–400	3.5	83	[13]
Mo_2N/γ-Al_2O_3,W_2N/γ-Al_2O_3,VN/γ-Al_2O_3	Oleic acid Canola oil	380–410	7.15	100	[19]
MoN/Al_2O_3, $CoMoN/Al_2O_3$, MoN/SBA15, CoMoN/SBA15	Guaiacol	300	5	66	[29]
$NiMo$–γ-Al_2O_3, Pd/γ-Al_2O_3, sulfided CoMo/γ-Al_2O_3, Ni/SiO_2–Al_2O_3, Pt/γ-Al_2O_3, Ru/Al_2O_3	Soybean oil	400	9.2	92.9	[30]
CoMo/Al_2O_3	Sunflower oil	380	4–6	100	[31]
Sulfided MoO_3/CoO/MCM-41	Rapeseed oil	300, 320	2–11	100	[32]
Sulfided NiMo/Al_2O_3 CoMo/Al_2O_3, NiW/Al_2O_3, NiMo/B_2O_3–Al_2O_3	Waste cooking oil	350	5	99	[33]
NiCo/γ-Al_2O_3	FAME derived from jatropha oil	300–400	2	78	Present study
NiCo/SiO_2				76	

comparison of the present study with literature. The major advantage of the present study is the execution of hydrotreatment of FAME at a comparatively lower hydrogen pressure (2 MPa) with a good FAME conversion.

Conclusion

Diesel range hydrocarbons (C12–C20) were produced by the hydrotreatment of jatropha FAME using reduced γ-Al_2O_3 and SiO_2 supported NiCo bimetallic catalysts. The hydrotreatment of jatropha oil derived FAME has been successfully carried out and a maximum conversion of 78.2 and 76.1 % were obtained for NiCo/γAl_2O_3 and NiCo/SiO_2, respectively, under the reaction conditions of 2 MPa and 400 °C. Diesel range hydrocarbons were obtained with a maximum selectivity of 79 and 73 % for NiCo/γAl_2O_3 and NiCo/SiO_2, respectively, at 400 °C. The reactant conversion was almost stable for continuous 5 h of reaction. Based on the product distribution studies, for both NiCo/γAl_2O_3 and NiCo/SiO_2, the major products formed were C15–C18 hydrocarbons and so it can be concluded that the reaction was proceeded through both hydrodeoxygenation and hydrodecarboxylation. Reduced metals (Ni, Co) activated H_2 spill over to adsorbed oxygen of the FAME resulting C-O bond cleavage.

References

1. Hari TK, Yaakob Z, Binitha NN (2015) Aviation biofuel from renewable resources: routes, opportunities and challenges. Renew Sustain Energy Rev 42:1234–1244
2. Zuo H, Liu Q, Wang T, Ma L, Zhang Q, Zhang Q (2012) Hydrodeoxygenation of methyl palmitate over supported Ni catalysts for diesel-like fuel production. Energy Fuels 26:3747–3755
3. Li K, Wnag R, Chen J (2011) Hydrodeoxygenation of Anisole over Silica-Supported Ni_2P, MoP, and NiMoP Catalysts. Energy Fuels 25:854–863
4. Bezergianni S, Kalogianni A, Dimitriadis A (2012) Catalyst evaluation for waste cooking oil hydroprocessing. Fuel 93:638–641
5. Grilc M, Likozar B, Levec J (2014) Hydrodeoxygenation and hydrocracking of solvolysed lignocellulosic biomass by oxide, reduced and sulphide form of NiMo, Ni, Mo and Pd catalysts. Appl Catal B 150–151(5):275–287
6. Grilc M, Veryasov G, Likozar B, Jesih A, Levec J (2015) Hydrodeoxygenation of solvolysed lignocellulosic biomass by unsupported MoS_2, MoO_2, Mo_2C and WS_2 catalysts. Appl Catal B 163:467–477
7. Grilc M, Likozar B, Levec J (2014) Hydrotreatment of solvolytically liquefied lignocellulosic biomass over $NiMo/Al_2O_3$ catalyst: reaction mechanism, hydrodeoxygenation kinetics and mass transfer model based on FTIR. Biomass Bioenergy 63:300–312
8. Larabi C, Al Maksoud W, Szeto KC, Garron A, Arquilliere PP, Walter JJ, Santini CC (2015) Multifunctional heterogeneous catalyst for one step transformation of lignocellulosic biomass into low oxygenated hydrocarbons. Appl Catal B 495:162–172
9. Santillan-Jimenez E, Morgan T, Lacny J, Mohapatra S, Crocker M (2013) Catalytic deoxygenation of triglycerides and fatty acids to hydrocarbons over carbon-supported nickel. Fuel 103:1010–1017
10. Liu C, Liu J, Zhou G, Tian W, Rong L (2013) A cleaner process for hydrocracking of jatropha oil into green diesel. J Taiwan Inst Chem Eng 44:221–227
11. Dundich VO, Khromova SA, Ermakov DY, Lebedev MY, Novopashina VM, Sister VG et al (2010) Nickel catalysts for the hydrodeoxygenation of biodiesel. Kinet Catal 51:704–709
12. Liu J, Fan K, Tian W, Liu C, Rong L (2012) Hydroprocessing of Jatropha oil over $NiMoCe/Al_2O_3$ catalyst. Int J Hydrog Energy 37:17731–17737
13. Liu J, Liu C, Zhou G, Shen S, Rong L (2012) Hydrotreatment of Jatropha oil over $NiMoLa/Al_2O_3$ catalyst. Green Chem 14:2499–2505
14. Ardiyanti AR, Khromova SA, Venderbosch RH, Yakovlev VA, Melián-Cabrera IV, Heeres HJ (2012) Catalytic hydrotreatment of fast pyrolysis oil using bimetallic Ni–Cu catalysts on various supports. Appl Catal A 449:121–130
15. Mohanty S, Mouli KC, Soni K, Adjaye J, Dalai AK (2012) Catalytic hydrotreatment using NiMo_MAS catalysts synthesized from ZSM-5 nano-clusters. Appl Catal A 419–420:1–12
16. Wang C, Liu Q, Song J, Li W, Li P, Xu R, Ma H, Tian Z (2014) High quality diesel-range alkanes production via a single-step hydrotreatment of vegetable oil over Ni/zeolite catalyst. Catal Today 234:153–160
17. Pinto F, Varela FT, Goncalves M, Andre RN, Costa P, Mendes B (2014) Production of bio-hydrocarbons by hydrotreating of pomace oil. Fuel 116:84–93
18. Liu Q, Zuo H, Wang T, Ma L, Zhang Q (2013) One-step hydrodeoxygenation of palm oil to isomerized hydrocarbon fuels over Ni supported on nano-sized SAPO-11 catalysts. Appl Catal A 468:68–74
19. Monnier M, Sulimma H, Dalai A, Caravaggio G (2010) Hydrodeoxygenation of oleic acid and canola oil over alumina-supported metal nitrides. Appl Catal A 382:176–180
20. Wang X, Wang F, Chen M, Ren J (2005) Studies on nickel based bimetallic catalysts for hydrodeoxygenation. J Fuel Chem Technol 33:612–616
21. Assaf PGM, Nogueira FGE, Assaf EM (2013) Ni and Co catalysts supported on alumina applied to steam reforming of acetic acid: representative compound for the aqueous phase of bio-oil derived from biomass. Catal Today 213:2–8

22. Pudukudy M, Yaakob Y, Akmal ZS (2015) Direct decomposition of methane over SBA-15 supported Ni, Co and Fe based bimetallic catalysts. Appl Surf Sci 330:418–430
23. Leng S, Wang X, He X, Liu L, Liu Y, Zhong X, Zhuang G, Wang J (2013) NiFe/γ-Al$_2$O$_3$: a universal catalyst for the hydrodeoxygenation of bio-oil and its model compounds. Catal Commun 41:34–37
24. Wang L, Murata K, Inaba M (2004) Development of novel highly active and sulphur-tolerant catalysts for steam reforming of liquid hydrocarbons to produce hydrogen. Appl Catal A 257:43–47
25. Bona S, Guillén P, Alcalde JG, García L, Bilbao R (2008) Chem Eng J 137:587
26. Luo N, Ouyang K, Cao F, Xiao T (2010) Hydrogen generation from liquid reforming of glycerin over Ni–Co bimetallic catalyst. Biomass Bioenergy 34:489–495
27. Sengupta S, Ray K, Deo G (2014) Effects of modifying Ni/Al2O3 catalyst with cobalt on the reforming of CH4 with CO2 and cracking of CH$_4$ reactions. Int J Hydrog Energy 39:11462–11472
28. Bortolozzi JP, Gutierrez LB, Ulla MA (2013) Synthesis of Ni/Al$_2$O$_3$ and Ni–Co/Al$_2$O$_3$ coatings onto AISI 314 foams and their catalytic application for the oxidative dehydrogenation of ethane. Appl Catal A 452:179–188
29. Ghampson IT, Sepúlveda C, Garcia R, Fierro JLG, Escalona N, DeSisto WJ (2012) Comparison of alumina- and SBA-15-supported molybdenum nitride catalysts for hydrodeoxygenation of guaiacol. Appl Catal A 435–436:51–60
30. Veriansyah B, Han JY, Kim SK, Hong S-A, Kim YJ, Lim JS, Shu Y-W, Oh S-G, Kim J (2012) Production of renewable diesel by hydroprocessing of soybean oil: effect of catalysts. Fuel 94:578–585
31. Krar M, Kovacs S, Kalló D, Hancsok J (2010) Fuel purpose hydrotreating of sunflower oil on CoMo/Al$_2$O$_3$ catalyst. Bioresour Technol 101:9287–9293
32. Kubicka D, Bejblova M, Vlk J (2010) Conversion of vegetable oils into hydrocarbons over CoMo/MCM-41 catalysts. Top Catal 53:168–178
33. Toba M, Abe Y, Kuramochi H, Osako M, Mochizuki T, Yoshimura Y (2011) Hydrodeoxygenation of waste vegetable oil over sulfide catalysts. Catal Today 164:533–537